ELSEVIER

Contents lists available at ScienceDirect

Environmental Modelling and Software

journal homepage: www.elsevier.com/locate/envsoft





Advancing the SWAT model to simulate perennial bioenergy crops: A case study on switchgrass growth

Sijal Dangol^a, Xuesong Zhang^{b,*}, Xin-Zhong Liang^a, Elena Blanc-Betes^c

- ^a Department of Atmospheric and Oceanic Science, University of Maryland, College Park, MD, 20742, USA
- ^b USDA-ARS Hydrology and Remote Sensing Laboratory, Beltsville, MD, 20705, USA
- ^c Center for Advanced Bioenergy and Bioproducts Innovation University of Illinois at Urbana-Champaign, Urbana, IL, 61801, USA

ARTICLE INFO

Handling editor: Daniel P Ames

Keywords:
Biomass production
DAYCENT
Vegetation growth
root:shoot ratio
SWAT
SWAT-GRASS
Switchgrass

ABSTRACT

Although the Soil and Water Assessment Tool (SWAT) model has been widely used to assess the environmental impacts of growing perennial grasses for bioenergy production, its utility is limited by not explicitly accounting for shoot and root biomass development. In this study, we integrated the DAYCENT model's grass growth algorithms into SWAT (SWAT–GRASS_D) and further modified it by considering the impact of leaf area index (LAI) on potential biomass production (SWAT–GRASS_M). Based on testing at eight sites in the US Midwest, we found that SWAT–GRASS_M generally outperformed SWAT and SWAT–GRASS_D in simulating switchgrass biomass yield and the seasonal development of LAI. Additionally, SWAT–GRASS_M can more realistically represent root development, which is key for the allocation of accumulated biomass and nutrients between aboveground and belowground biomass pools. These improvements are critical for credible assessment of agronomic and environmental impacts of growing perennial grasses for biomass production.

Software availability

Software: Algorithms to represent switchgrass as influenced by climate, nutrients, and water.

Description: Algorithms developed, tested, and presented as part of this work. The code is embedded in the SWAT and SWAT-Carbon models.

Developer: Sijal Dangol and Xuesong Zhang. Contact address: xuesong.zhang@usda.gov.

Language: Fortran 95.

Availability: Freely available at https://sites.google.com/view/swat-carbon.

1. Introduction

The transition from fossil fuel to carbon-neutral or carbon-negative energy sources, such as bioenergy, has been incentivized through policies such as the Renewable Fuel Standard (RFS) established by the U.S. Energy Independence and Security Act (EISA) 2007 (Schnepf and Yacobucci, 2013; U.S. EPA, 2022). The wide use of grain crops for bioenergy production in the U.S. has raised serious concerns regarding the competition between food and fuel and detrimental environmental

impacts (Lark et al., 2022; Searchinger et al., 2008; Zhang et al., 2010). Perennial grasses have been recognized as potential resource to fulfill future EISA mandated cellulosic biofuel production, minimize conflicts with food production, reduce negative impacts on the environment, and mitigate regional climate change (Gelfand et al., 2013; LeDuc et al., 2017; National Research Council, 2009). In addition to bioenergy production, perennial grasses like switchgrass and miscanthus can serve as a means to sequestrate carbon (Clifton-Brown et al., 2007; Qin et al., 2012). The extensive root biomass and absence of tillage promote carbon sequestration in soil (Agostini et al., 2015; Anderson-Teixeira et al., 2009; Rasse et al., 2005). Although field experiments offer valuable insights to understand and quantify the environmental impacts of biofuel feedstock production, scaling up the results to regional, national, or global scales, requires modeling approaches. Therefore various models have been developed and applied to represent the vegetation growth processes of perennial grasses like switchgrass, miscanthus, and energycane (Cibin et al., 2016; Gopalakrishnan et al., 2012; He et al., 2022; Kiniry et al., 2008; Lee et al., 2012; Miguez et al., 2012). Existing models such as Daily CENTURY (DAYCENT), Soil and Water Assessment Tool (SWAT), DeNitrification-DeComposition (DNDC), Environmental Policy Integrated Climate (EPIC), Decision Support System for Agrotechnology Transfer DSSAT), Agricultural Land Management Alternatives with

E-mail address: xuesong.zhang@usda.gov (X. Zhang).

^{*} Corresponding author.

Numerical Assessment Criteria (ALMANAC), and BioCro have been tested and applied to estimate productivity and environmental consequences associated with cultivation of perennial grasses (Cibin et al., 2016; Davis et al., 2010; Kantola et al., 2022; Lee et al., 2012; Nocentini et al., 2015; Proulx et al., 2022; Sharara et al., 2020; Sinistore et al., 2015; Trybula et al., 2015). Given that most of those models operate at the field and regional scales, SWAT stands out with its unique capabilities to provide a thorough evaluation of the impacts on water budget and water quality at the watershed scale. However, the poor representation of the perennial crops limits its ability to reproduce biogeochemical processes, with potential implications on estimates of evapotranspiration fluxes, runoff, and discharge.

The SWAT plant growth sub-model and parameters have been extensively tested for food/feed crops like corn, soybean, wheat, barley, etc. (Gassman et al., 2010; Luo et al., 2008; Zhang et al., 2013), while few studies (Cibin et al., 2016; Nelson et al., 2006; Ng et al., 2010; Trybula et al., 2015) have evaluated its suitability to simulate perennial bioenergy crops. Switchgrass shows great potential as a bioenergy crop with relatively high productivity and different cultivars already available in the market for optimum allocation across climatic zones (Clifton-Brown et al., 2019; Larnaudie et al., 2022; Mehmood et al., 2017). Nonetheless, despite previous attempts, the lack of explicit representation of shoot and root growth is a major drawback of the SWAT (Zhang et al., 2011). Field observations have shown that root growth, in general, is influenced by temperature, moisture, and nutrient availability and exhibits large sensitivities to climatic conditions (Sainju et al., 2017).

In earlier studies involving switchgrass, plant growth parameters were parameterized for a lowland cultivar, Alamo, adapted to grow in wetter conditions (Trybula et al., 2015). For example, Srinivasan et al. (2010) adapted crop growth parameters for Alamo Switchgrass in large-scale bioenergy simulations to assess the environmental impacts of land use change. Trybula et al. (2015) then parameterized the SWAT crop growth parameters for an upland switchgrass cultivar adapted to grow in drier conditions, based on experimental field data, and improved the model representation of plant growth for perennials. Previous studies also parameterized switchgrass (both lowland and upland cultivars) in the EPIC model to evaluate the environmental impacts of cultivating switchgrass for bioenergy production (Egbendewe--Mondzozo et al., 2011, 2013). Note that SWAT employs a simplified vegetation growth sub-model adapted from EPIC (Williams et al., 1989). Therefore, the above studies, in general, used a single plant growth pattern for all plant types (forest, grass, and annual crops), which lacks representation of complex plant phenology, for example, growth of different plant compartments (root, shoot, leaf, etc.), carbon and nutrient dynamics between above and belowground pools (Luo et al., 2008). As such, further improvements of the SWAT vegetation growth sub-model are needed to characterize the behavior of perennial grass growth and provide assessment of hydrologic, nutrient, and carbon cycle responses to bioenergy feedstock production.

This study aims to enhance the SWAT plant growth sub-model to improve simulation of biomass production of perennial grass. We integrated the grass growth sub-model from DAYCENT into SWAT and referred to the new model as the SWAT-GRASS hereafter. The DAYCENT grass sub-model can simulate crop development, biomass production, and carbon and nutrient allocation to shoot and root as influenced by various elements such as climate, nutrient, and water availability (Parton et al., 1998). The model has been used to simulate biomass production of perennial grasses like switchgrass and miscanthus on the field and regional scale (Chen et al., 2021; Davis et al., 2010; Hudiburg et al., 2015, 2016). We evaluated the SWAT-GRASS model against the observed switchgrass biomass yield at multiple farm sites in Wisconsin, Michigan, and Illinois. The sites considered here represent both low and high productivity land areas that help assess the potential for sustainable bioenergy feedstock production. The improved representation of vegetation growth provides new features into the SWAT model for studying the watershed scale impact of growing perennial bioenergy crops on soil

organic matter, nutrient uptake, and water quality. The outcomes of this study will also be helpful in model development and application for different types of perennial grasses to generate more realistic information for understanding the sustainability issues related to bioenergy feedstock production.

2. Materials and methods

2.1. SWAT plant growth sub-model

The SWAT model utilizes a simplified plant growth sub-model based on the EPIC model for all plant types (annual crops, grass, and forest) to simulate plant growth based on accumulated heat units (Williams et al., 1989). The growth sub-model first simulates the potential plant biomass production under ideal conditions based on the radiation use efficiency coefficient and the intercepted photosynthetically active solar radiation. Then, it calculates the actual growth of the plant taking into account the influence of temperature, water, nitrogen, phosphorus, and aeration stress factors (Neitsch et al., 2011) as described in Appendix A.

The SWAT model determines the seasonal partitioning of plant biomass to root by a static root-shoot ratio (RSR) at the specific plant growth stage (Eq. (A.1)). Such simplified assumptions of plant root fraction could result in substantial differences in biomass yield of perennials and overall impact on hydrologic processes, water quality, and soil organic carbon. For example, the default values of root fraction at the planting (rsr1) and maturity (rsr2) are 0.2 and 0.4 respectively. Based on this assumption, about 60% of plant biomass would be available as yield at the early growing season and about 80% when harvested at the end of the growing season. This method does not consider the explicit allocation of accumulated biomass into shoot and root, nor the impact of climate conditions on root development. In addition, the simple RSR approach does not consider the fact that perennial grasses such as switchgrass and miscanthus translocate nutrients to root during the late growing season, which the plant remobilizes during the next growing season (Ashworth et al., 2017; Massey et al., 2020). Such nutrient cycling during different phases of plant growth reduces the plant nutrient stress, resulting in high biomass production even in low-productivity soil. Furthermore, the plant biomass death during senescence and subsequent return to soil is not well simulated in SWAT. For perennials, a fraction of biomass (generally 10%) dies off and is added to soil organic matter during dormancy in SWAT. However, SWAT does not account for the root and shoot biomass death separately during the growing season, which affects the soil organic matter dynamics.

2.2. DAYCENT grass growth sub-model

DAYCENT is a biogeochemical model that simulates the dynamics of carbon, nitrogen, phosphorous, and sulfur for grassland, agricultural land, forest, and savannas (Del Grosso et al., 2008; Parton et al., 1998). The model has separate plant production sub-models for grass/crop, forest, and savanna to predict biomass growth. Its grass growth sub-model, detailed in Metherell et al. (1993), accounts for the dynamic nature of biomass allocation to shoot and root based on plant growth stage, climatic conditions, and nutrient availability. DAYCENT also simulates shoot and root death and accounts for nutrient translocation within the plant. For instance, if water or nutrients are limited, the plant response would be to allocate more resources to roots (Davis et al., 2010; Kantola et al., 2022). In this study, we incorporated DAYCENT's grass sub-model (see details in Appendix B) into SWAT to create the SWAT–GRASS_D model.

2.3. Modifications to potential biomass production

DAYCENT uses a simplified approach to estimate the leaf area index as leaf area ratio (LAR) multiplied by total aboveground biomass. By

default, LAR is set to a constant value of 0.01 for all crops/grasses. However, LAR has been found to vary spatially (Zhang et al., 2018). The SWAT requires LAI to compute rainfall interception by the plant canopy and potential evapotranspiration (Neitsch et al., 2011), which subsequently affects plant water use. The use of a LAR coefficient for LAI development in DAYCENT could reduce the performance of the integrated model in simulating plant water use and biomass production (Zhang et al., 2018). Thus, the calculation of potential biomass production was further modified to incorporate the influence of seasonally varying leaf area on solar radiation intercepted by the perennial grasses. For this, an additional scaling factor, *laiprod*, used in the DAYCENT forest sub-model, is introduced in Eq. (B.1). The new equation is as follows:

$$tgprod = shwave \times T_{stress} \times SM_{stress} \times Sdlng \times CO2cpr \times biof \times laiprod \tag{1}$$

where, $tgprod\ (g\ C/m^2)$ is the potential biomass production on a given day, shwave is downwelling solar radiation (Lg/day), SM_{stress} is the soil moisture effect, T_{stress} is the temperature effect, Sdlng is the constraint on biomass production representing the seedling growth, CO2cpr is the effect of CO_2 concentration on biomass production, scenfrac represents the loss of biomass due to senescence, and biof is the effect of physical obstruction by standing dead biomass.

$$laiprod = 1 - exp(-k_l \times LAI)$$
 (2)

where, k_l is light extinction coefficient, and LAI is leaf area index calculated by SWAT as:

$$LAI_i = LAI_{i-1} + \Delta LAI_i \tag{3}$$

$$\Delta LAI_{i} = \left(fr_{LAImx,i} - fr_{LAImx,i-1}\right) \times LAI_{mx} \times \left(1 - exp\left(5 \times \left(LAI_{i-1} - LAI_{mx}\right)\right)\right) \tag{4}$$

where, ΔLAI_i is increment of leaf area index on day i, $fr_{LAImx,i}$ and $fr_{LAImx,i-1}$ are fraction of maximum leaf area index on day i and i-1, LAI_i and LAI_{i-1} are leaf area indices on day i and i-1, and LAI_{mx} is the maximum leaf area index for the plant.

The introduction of the scale factor laiprod was accompanied by the substitution of soil moisture stress (SM_{stress}) in Eq. (B.1) with SWAT estimated plant water stress $(Stress_w)$. $Stress_w$ is proportional to the ratio of actual plant water uptake to potential evapotranspiration (Eq. (A.4)), which is considered to be a good measure of water stress impact on biomass production (Zhang et al., 2018). The newly integrated SWAT–GRASS model with these modifications is referred to as SWAT–GRASS_M.

2.4. Field experimental sites

The SWAT and two versions of SWAT–GRASS models were evaluated at five Great Lakes Bioenergy Research Center (GLBRC) field sites in Michigan and Wisconsin (Escaban, Hancock, Rhinelander, Luxarbor, and Lakecity) and three field sites across Illinois (Fairfield, Orr, and Dekalb; selected from Arundale et al. (2014)) (referred to as AR sites) (Fig. 1). For these sites, biomass yield data for the Cave-in-Rock cultivar were available. The average annual precipitation and temperature range between 766 and 1044 mm and 6 and 13 °C, respectively, across all eight field sites (Table 1 and SI Figure S1). In general, switchgrass biomass yield was higher in sites with warmer temperatures and higher precipitation (Hartman et al., 2012; Li et al., 2022).

2.5. Model setup

The SWAT and SWAT-GRASS models were setup for watersheds (within which the field sites were located) using the geospatial inputs listed in Table 2. In SWAT, Hydrologic Response Units (HRUs) are

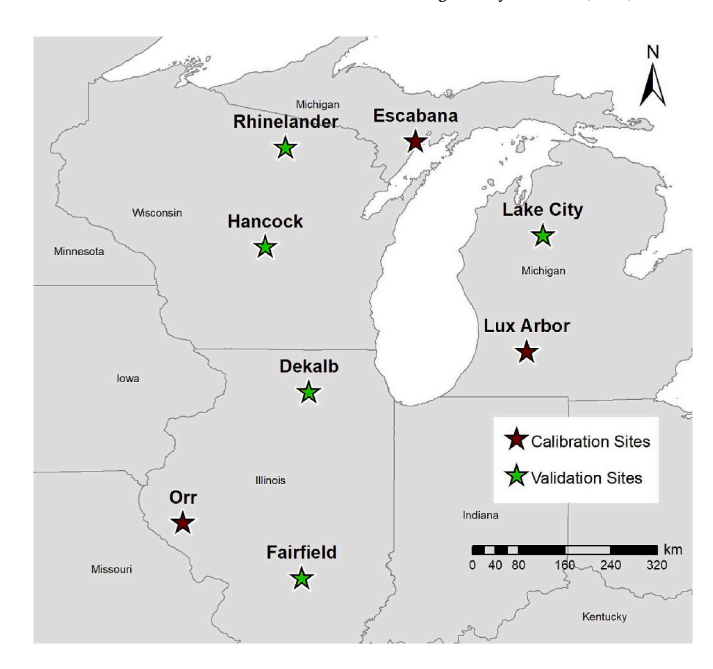


Fig. 1. Location of GLBRC and AR field sites.

generated by the unique combination of land use, soil, and slope within a watershed. Here, we use the HRUs collocated with the switchgrass field sites and further assign detailed management operations. The fieldlevel management operations were scheduled by date, consisting of planting, fertilizer application, and harvesting, as detailed by Arundale et al. (2014) for the AR sites and by Martinez-Feria and Basso (2020) for the GLBRC sites (Table 1). Switchgrass was planted between May and June and harvested every subsequent year between October and November. The fertilizer application rates were based on Arundale et al. (2014) and Martinez-Feria and Basso (2020). For additional information on experimental design, see GLBRC data catalog at https://data.sustai nability.glbrc.org/datatables and Arundale et al. (2014). The harvesting efficiency (HARVEFF) of 0.8 was used based on settings from Ng et al. (2010). The upland switchgrass plant growth parameters for SWAT were adopted from the study by Cibin et al. (2016). For SWAT-GRASS, upland switchgrass growth parameters were adopted from Davis et al. (2010). The switchgrass growth parameters used in SWAT and SWAT-GRASS are provided in SI Tables S1 and S2, respectively.

In the natural grassland ecosystem, the primary source of nitrogen is wet and dry atmospheric deposition (Del Grosso et al., 2008). The atmospheric deposition of nitrogen tends to increase biomass production in nitrogen-limited watersheds (Fernández-Martínez et al., 2017; Sullivan and Gao, 2016). Given the relevance of atmospheric nitrogen deposition on biomass production of grass, the wet and dry atmospheric deposition rates reported by National Atmospheric Deposition Program (NADP) (NADP, 2022) were used. The total annual wet and dry nitrogen atmospheric deposition was computed for each site. The SWAT weather data inputs were obtained from North American Land Data Assimilation System (NLDAS-2) dataset (Xia et al., 2009). The model simulations for GLBRC sites and AR sites were conducted from 2013 to 2021 and from 2005 to 2009/2011, respectively.

2.6. Model calibration and validation

We simultaneously calibrate the three models at multiple sites to ensure parameter generality for testing sites. This approach helps in the generalization of switchgrass growth parameters for application across large areas (Zhang et al., 2008). The field-level biomass yield data from GLBRC field sites (Martinez-Feria and Basso, 2020) and Arundale et al. (2014) (Table 1) were used to optimize and evaluate the SWAT and SWAT–GRASS for simulating upland switchgrass biomass yield. The

Table 1
Field sites used to calibrate and validate SWAT and SWAT–GRASS plant growth parameters for switchgrass.

Data source	Location	Latitude, Longitude	Soil taxonomic class	Data record length	Annual Precipitation (mm)	Annual Average Temperature (°C)
GLBRC	Rhinelander, Wisconsin	45.6656, -89.2180	Sandy loam	2014–2021	808	5.8
	Hancock, Wisconsin	44.1129, -89.5334	Sand	2014–2021	838	8.0
	*Escabana, Michigan	45.7627, -87.1877	Fine sandy loam	2014–2021	766	6.5
	Lake City, Michigan	44.2961, -85.1996	Sand	2014–2021	852	7.8
	*Lux Arbor, Michigan	42.4764, -85.4519	loam	2014–2021	933	9.5
Arundale et al. (2014)	Fairfield, Illinois	38.95, -88.96	Silt loam	2006–2009	1044	13.3
	Dekalb, Illinois	41.85, -88.85	Silt loam	2006–2011	935	10.2
	*Orr, Illinois	39.81, -90.82	Silt loam	2006–2011	973	12.5

Note: * indicates the sites that were used for model calibration. The three sites selected here represent the two ends of the gradient from the cooler, drier, and low productivity areas Escabana and Lux Arbor sites to the warmer, wetter, and high productivity Orr site.

Table 2Geospatial inputs used for SWAT setup.

Data	Resolution	Source
Meteorology data	0.125° × 0.125°	NLDAS-2 (Xia et al., 2009)
Digital Elevation Model (DEM)	90 m × 90 m	Shuttle Radar Topography Mission (SRTM) (Jarvis et al., 2008)
Land Use Soil Property	30 m × 30 m 1:24,000	USDA NASS Cropland Data Layer (2008) Soil Survey Geographic database (SSURGO) (USDA-NRCS, 1994)

observed biomass yields from three field sites (Escabana, Orr, and Luxarbor) were used to calibrate the models. By including these sites, we aimed to ensure that the optimized model parameters would account for the variability in temperature, precipitation, and soil productivity. Sensitivity analysis and calibration of plant growth parameters were carried out using the Sequential Uncertainty Fitting algorithm version 2 (SUFI-2) procedure in SWAT-CUP (Abbaspour et al., 2015). The Kling–Gupta efficiency criterion (*KGE*) (Gupta et al., 2009) was used as the objective function for model calibration. *KGE* ranges from $-\infty$ to 1, with a higher value of *KGE* indicating better model performance. We further evaluated the model performance for simulated yield using percent bias (*PBIAS*), correlation coefficient (*R*), and root mean square error (*RMSE*) (Moriasi et al., 2007).

The SWAT plant growth parameters selected for sensitivity analysis were based on prior studies (Cibin et al., 2016; Ng et al., 2010; Trybula et al., 2015) and are listed in SI Table S3. The SWAT–GRASS plant growth parameters selected for the sensitivity analysis were based on previous studies (Chamberlain et al., 2011; Davis et al., 2010; Lee et al., 2012) and are listed in SI Table S4. The sensitivity analysis, as described above for SWAT, was implemented for SWAT–GRASS as well.

To establish confidence in the SWAT–GRASS model and the optimized switchgrass growth parameters, we validated the model simulated yield with independent biomass yield datasets for the remaining five field sites (Hancock, Rhinelander, Lake City, Fairfield, and Dekalb) from the GLBRC and AR sites that span across a range of climatic conditions in different geographical regions (Illinois, Michigan, and Wisconsin) (Fig. 1). We assessed the model prediction uncertainty by estimating the P-factor and R-factor using SUFI-2. The P-factor quantifies the fraction of observed data that falls within the 95% prediction uncertainty (95PPU) band, ranging from 0 to 1. The R-factor is the ratio between the width of the 95PPU band and the standard deviation of the observed data, with values ranging from 0 to infinity. The P-factor close to 1 and the R-factor close to 0 indicates low prediction uncertainty.

3. Results and discussion

3.1. Sensitivity analysis

Tables S3 and S4 list the SWAT and SWAT-GRASS plant growth parameters used for sensitivity analysis. Using global sensitivity in SUFI-2, the most sensitive parameters were identified and adjusted through the calibration process with final optimal values shown in Tables 3 and 4. The SWAT model was found to be sensitive to BIO_E, T_OPT, T_BASE, RSR2C, LAIMX2, and nutrient fraction parameters for nitrogen at three stages of plant growth (i.e., PLTNFR1, PLTNFR2, and PLTNFR3) (SI Figure S2), which is consistent with the sensitivity analysis results from Trybula et al. (2015). PLTNFR2 was one of the most sensitive parameters followed by PLTNFR1, which indicates that plant nitrogen cycling had a major impact on SWAT-simulated switchgrass yield. PLTNFRs control the amount of nitrogen in plant biomass that subsequently determines the plant nitrogen demand and plant nutrient stress during plant growth. BIO E (radiation use efficiency) determines the daily biomass production. LAIMX2 determines the LAI development and affects plant water demand and photosynthetically active radiation. TOPT and TBASE affect plant temperature stress and the timing of plant maturity. It is worth noting that the adjustment of T OPT and T BASE to ca. 20.8 and 9.7 °C from their default values of 25 and 10 °C, respectively, intensified the crop growth within a narrower temperature range, specifically

Table 3Calibrated SWAT plant growth parameters for switchgrass biomass yield.

		0 1 0		
ID	Parameters	Description	Range used	Fitted value
1	r_T_OPT	The optimal temperature for plant growth (°C)	$\pm 20\%$	-17%
2	r_T_BASE	Base temperature for plant growth (°C)	$\pm 20\%$	-3%
3	r_BIO_E	Radiation use efficiency (biomass/ energy ratio)	±40%	33%
4	$r_PLTNFR1$	Plant nitrogen fraction at emergence	$\pm 50\%$	17%
5	r_PLTNFR2	Plant nitrogen fraction at 50% maturity	±50%	26%
6	r_PLTNFR3	Plant nitrogen fraction at maturity	$\pm 50\%$	47%
9	v_LAIMX2	Fraction of the leaf area index	0.8 to	0.921
		corresponding to the 2nd. point on the optimal leaf area development curve	0.95	
10	v_RSR2C	Root fraction at the end of the growing season	0.35 to 0.60	0.398

Note: Here r and v represent the relative change and replacement of model parameters by adjusted value.

Table 4
Calibrated SWAT–GRASS plant growth parameters for switchgrass biomass yield.

ID	ID Parameters	Description		Fitted Values	
			used	SWAT-GRASS _D	SWAT-GRASS _M
1	r_T_OPT	optimal temperature for plant growth (°C)	±40%	-14%	7%
2	$r_{-}T_{-}BASE$	base temperature for plant growth (°C)	$\pm 40\%$	23%	24%
3	v_DLAI	fraction of growing season when leaf area starts declining	0.8 to 1.2	1.045	1.014
4	v_LAIMX1	fraction of the max. leaf area index corresponding to the 1st. point on the optimal leaf area development curve	0.05 to 0.10	-	0.100
5	r_FRGRW1	fraction of the plant growing season corresponding to the 1st. point on the optimal leaf area development curve		-	5%
6	r_FRGRW2	fraction of the plant growing season corresponding to the 2nd. point on the optimal leaf area development curve		-	0.7%
7	r_ppdf(2)	maximum temperature for plant growth (°C)	$\pm 30\%$	11%	-0.8%
8	r_ppdf(3)	left curve shape parameter that controls temperature effect on plant growth		12%	13%
9	$r_ppdf(4)$	right curve shape parameter that controls temperature effect on plant growth	$\pm 30\%$	21%	-5%
10	v_prdx	potential aboveground monthly biomass production (g C/m ²)	0.5 to 4.0	2.809	2.161
11	v_riint	root impact intercept that controls the impact of root biomass on nutrient availability	0.4 to 1.0	0.487	0.834
12	v_cfrtcn(1)	maximum fraction of carbon allocated to roots under maximum nutrient stress	0.5 to 0.7	0.502	0.630
13	v_cfrtcn(2)	minimum fraction of carbon allocated to roots in the absence of nutrient stress	0.2 to 0.3	0.334	0.357
14	v_cfrtcw(1)	minimum fraction of carbon allocated to roots under maximum water stress	0.4 to 0.7	0.618	0.599
15	v_cfrtcw(2)	minimum fraction of carbon allocated to roots in the absence of water stress	0.2 to 0.3	0.355	0.308
16	v_crprtf(1)	fraction of N transferred to a vegetation storage pool at death	0.50 to 0.95	0.861	0.791
17	v_pramn (1,1)	minimum aboveground C:N ratio with zero biomass	15 to 25	-	17.097
18	ν_pramn (1,2)	minimum aboveground C:N ratio with biomass equal to biomax	40 to 80	74.355	68.158
19	r_pramx (1,2)	maximum aboveground C:N ratio with biomass equal to biomax	$\pm 20\%$	-	13%
20	v_prbmn (1,1)	intercept for calculating the minimum C:N ratio for belowground biomass as a linear function of annual precipitation	40 to 60	42.239	49.864
21	v_prbmn (1,2)	slope for calculating the minimum C:N ratio for belowground biomass as a linear function of annual precipitation		-	0.113
22	r_clsgres	late season crop growth restriction factor	$\pm 20\%$	-10%	-2%
23	r_biomax	biomass level above which the minimum and maximum C:E ratios of new shoot increments equal pramn (;,2) and pramx (;,2) respectively (g biomass/m²)	±30%	-	1.2%
24	v_pltmrf	plant mature root fraction	0.8 to 1.0	0.955	0.987
25	v_fallrt	fall rate (fraction of standing dead which falls each month)	0.005 to 0.15	0.009	0.096

Note: Here r and v represent the relative change and replacement of model parameters by adjusted value.

between T_BASE to 2 \times T_OPT - T_BASE . This adjustment resulted in higher sensitivity of biomass production to temperature stress.

Both SWAT-GRASS_D and SWAT-GRASS_M were found to be sensitive to T_OPT, T_BASE, ppdf(2), ppdf(3), ppdf(4), prdx, riint, cfrtcn(2), crptf (1), clsgres, pltmrf, and fallrt (SI Figures S3 and S4). The parameters pramn(1,2) and pramx(1,2) regulate the C:N ratio of aboveground and belowground biomass. $T_{.}OPT$ and $T_{.}BASE$ in conjunction with ppdf(2), ppdf(3), and ppdf(4) determine the plant's response to changes in atmospheric temperature and control the timing of plant maturity. prdx is the maximum potential monthly biomass production rate that affects daily biomass production. cfrtcn(2) affects the biomass allocation to roots under nitrogen stress. crptf(1) determines the nitrogen translocation from the shoot to the root during the late growing season. clsgres regulates the late-season growth of the plant. pltmrf is the planting month reduction factor that scales the plant growing from seedlings. fallrt regulates the rate at which standing dead biomass is transferred to surface litter. For SWAT-GRASS_D, the most sensitive parameter was fallrt, followed by T BASE, DLAI, prdx, T OPT, crprtf(1), ppdf(2), and pltmrf (SI Figure S3). Similarly, for SWAT-GRASS_M, the most sensitive parameter was prdx, followed by fallrt, DLAI, T_BASE, T_OPT, ppdf(2), and FRGRW1 (SI Figure S4).

These results indicate that the parameters regulating the plant nitrogen cycle, such as plant nitrogen use efficiency and the impact of nitrogen stress on biomass production, are critical factors in determining biomass yield in SWAT. Meanwhile, parameters that regulate the plant growth response to temperature changes and plant growth processes during senescence were critical factors for biomass yield in SWAT–GRASS_D and SWAT–GRASS_M. Overall, these findings provide insights into the key parameters that should be considered when predicting

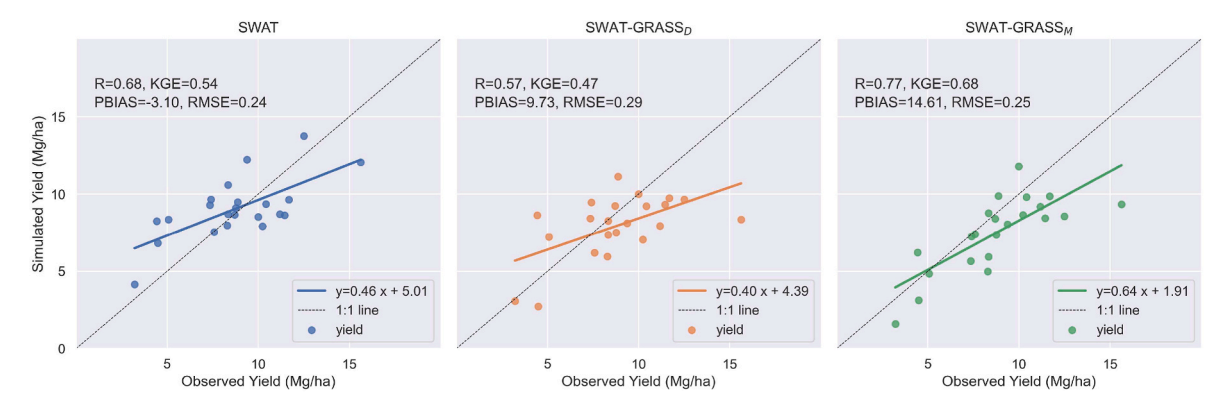
biomass production using SWAT, SWAT–GRASS $_{\mathrm{D},}$ and SWAT–GRASS $_{\mathrm{M}}$ models.

3.2. Model calibration and validation for biomass simulation

3.2.1. Calibration

SWAT, SWAT–GRASS_D, and SWAT–GRASS_M were able to capture the variability in biomass yield with $R \geq 0.5$ (Fig. 2). The *PBIAS* was found to be within $\pm 25\%$ and $KGE \geq 0.45$ for all three models (Fig. 2), indicating low bias in model performance. These results demonstrate the ability of all three models to reasonably simulate biomass yield across the three calibration sites. Among the three models, SWAT achieved the least bias, while SWAT–GRASS_M performed the best in terms of capturing the variability in observed biomass yield. SWAT–GRASS_M exhibited improved accuracy in simulating the standard deviation of observed biomass yield across the calibration sites (2.4 Mg/ha vs. observed standard deviation of 2.9 Mg/ha), while SWAT (2.0 Mg/ha) and SWAT–GRASS_D (2.1 Mg/ha) underestimated variability. SWAT–GRASS_D performed the least in terms of R, KGE, and RMSE. With the modifications introduced in SWAT–GRASS_M, the SWAT–GRASS_M shows considerable improvement in simulating biomass yield.

At the individual site level, the performance metrics of the three models vary across the field sites (Fig. 3). For example, both SWAT–GRASS $_{\rm D}$ and SWAT–GRASS $_{\rm M}$ outperformed SWAT in simulating biomass yield for Escabana in terms of R and KGE. Likewise, at Lux Arbor, SWAT–GRASS $_{\rm D}$ performed modestly better in terms of KGE, while SWAT–GRASS $_{\rm M}$ exhibited substantial improvement in terms of both R and KGE compared to SWAT. On the other hand, at Orr, SWAT–GRASS $_{\rm D}$ performed poorly than SWAT in terms of KGE, RMSE, and PBIAS, and



 $\textbf{Fig. 2.} \ \ \, \textbf{SCatter plots of SWAT, SWAT-GRASS}_{D,} \ \, \textbf{and SWAT-GRASS}_{M} \ \, \textbf{simulated and observed annual dry weight biomass yield for all calibration sites}.$

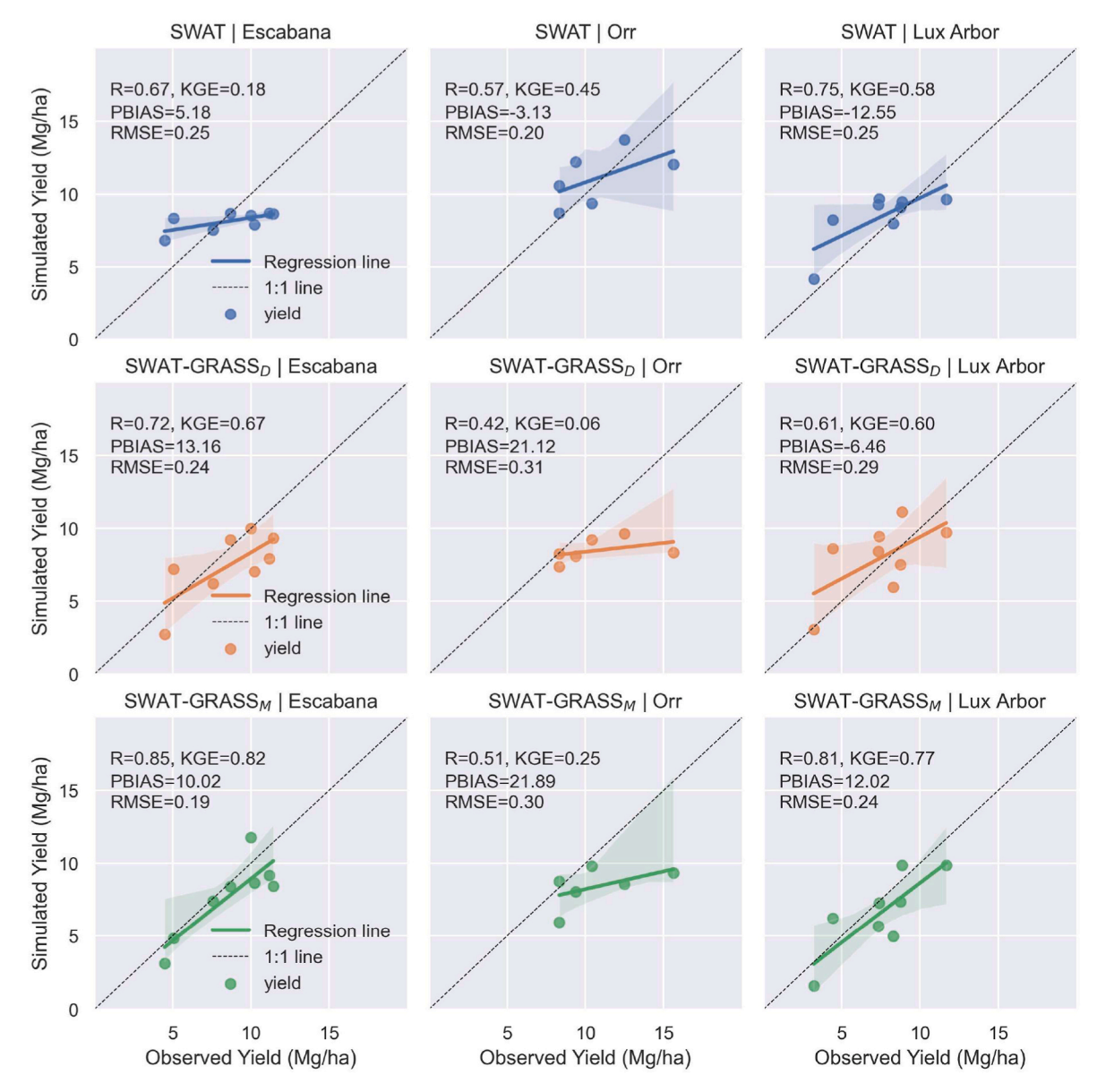


Fig. 3. Scatter plots of SWAT, SWAT-GRASS_D, and SWAT-GRASS_M simulated and observed annual dry weight biomass yield for individual calibration field sites.

simulated biomass yield substantially worse than $SWAT-GRASS_M$, which still had lower KGE and RMSE than SWAT. In general, the calibration results show that none of the three models can consistently

outperform the other two models in terms of all metrics and at all sites, indicating that each of these three models has their own strengths and weaknesses. This result also demonstrates that the plant growth

processes are complex, and it is difficult to identify a single optimum algorithm.

3.2.2. Validation

Across the five validation sites, SWAT, SWAT–GRASS_D, and SWAT–GRASS_M simulated average annual biomass yields of 8.9, 7.7, and 7.8 Mg/ha, respectively, compared to the observed value of 7.1 Mg/ha. SWAT performed satisfactorily with a *KGE* of 0.37 and a *PBIAS* of -25.77%. In comparison, SWAT–GRASS_D achieved a higher *KGE* (0.46) and reduced *PBIAS* (-8.67%) and *RMSE* (0.45) compared to SWAT. SWAT–GRASS_M modestly outperformed SWAT–GRASS_D, with an *R* of 0.55, *RMSE* of 0.44, and a *KGE* of 0.47 (Fig. 4). We found that the model performance was substantially influenced by the underestimation of two instances of high yields (16 Mg/ha) observed at Fairfield in 2007 and 2008. Assuming these points as outliers, SWAT–GRASS_M achieved a substantial improvement in the simulation of biomass yield compared to both SWAT and SWAT–GRASS_D in terms of *R* (0.58 vs 0.42 and 0.51), *RMSE* (0.42 vs 0.53 and 0.44), and *KGE* (0.54 vs 0.28 and 0.48), respectively.

Fig. 5 compares the observed and simulated biomass yield at each validation field site and demonstrates that model performance varied considerably across validation field sites (Hancock, Rhinelander, Lake City, Fairfield, and Dekalb) and between the models during validation. The observed mean dry weight biomass yield varies considerably across the field sites, ranging from 3.6 to 13.8 Mg/ha. In general, the three models simulated mean biomass yield well at Rhinelander, Lake City, and Fairfield, but showed large bias at Hancock and Dekalb (Table S5). The varied performance of the models across different sites could be caused by the accuracy of observed yield data and other input data, such as soil properties and management practices.

Across the five validation sites, SWAT– $GRASS_M$ provided comparable or improved performance when compared to SWAT and SWAT– $GRASS_D$ in terms of R and KGE, across the validation sites (Fig. 5). For most sites, both SWAT– $GRASS_D$ and SWAT– $GRASS_M$ demonstrate good performance as indicated by R and KGE values, except for Fairfield and Hancock. It is also worth noting that SWAT– $GRASS_M$ achieved comparable PBIAS compared with SWAT and SWAT– $GRASS_D$ at Rhinelander, and Fairfield, and lower PBIAS at Hancock, Lake City, and Dekalb. Meanwhile, SWAT achieved lower RMSE at Lake City and Fairfield compared with SWAT– $GRASS_D$ and SWAT- $GRASS_M$. Similar to the calibration results, although none of the three models can outperform the other two in terms of all metrics and at all sites, SWAT– $GRASS_M$ provided the best overall performance.

3.2.3. Uncertainty analysis

We calculated the P-factor and R-factor for biomass yield at the eight field sites using the final calibrated parameter ranges. The values of P-factor and R-factor are listed in SI Table S6. The P-factor ranged from 0.13 to 0.63, 0.38 to 0.67, and 0.38 to 0.83 for SWAT, SWAT–GRASS $_{\rm D}$,

and SWAT–GRASS $_{\rm M}$, respectively. The R-factor ranged from 0.62 to 1.11, 0.97 to 2.18, and 1.73 to 3.10 for SWAT, SWAT–GRASS $_{\rm D}$, and SWAT–GRASS $_{\rm M}$, respectively. In general, SWAT–GRASS $_{\rm M}$ and SWAT–GRASS $_{\rm D}$ obtained P-factor values closer to 1 (or the fraction of observations covered in the 95% confidence interval) than SWAT. Notably, the changes made in SWAT–GRASS $_{\rm M}$ helped it obtain slightly greater P-factor and R-factor values than SWAT–GRASS $_{\rm D}$. These results indicate that the modification of crop growth made the model to better represent the uncertainties associated with switchgrass yield prediction.

3.3. Assessment of model simulated leaf area index

LAI is an important plant parameter for all three models for simulating plant growth. As measured LAI data for the field sites were not available, we used regression-estimated LAI to qualitatively assess the model ability to accurately represent LAI dynamics. We compared the seasonal development of LAI simulated by SWAT, SWAT–GRASS $_{\rm D}$, and SWAT–GRASS $_{\rm M}$ against the regression-estimated seasonal LAI for upland switchgrass by Madakadze et al. (1998), hereafter referred to as CTRL (Fig. 6). The regression model is based on LAI data measured until the late summer months. Therefore, to ensure consistency, we qualitatively evaluate the simulated LAI values only up to August.

SWAT and SWAT-GRASS_D exhibited earlier and more rapid LAI development than the CTRL data, while $SWAT-GRASS_M$ simulates lower and gradual LAI development from mid-spring months that matches well with CTRL. The broad temperature ranges for SWAT-GRASS_D within which biomass production can take place, allow for plant growth in early spring that contribute to early LAI development. In contrast, the relatively high T BASE and narrow temperature range for plant growth $(T_BASE = 12.4, ppdf(2) = 49.6, and ppdf(4) = 2.39)$ in SWAT-GRASS_M limited plant growth in cooler early spring months. All three models simulate a rapid increase in LAI during the early summer months before reaching its peak value in July, in alignment with the CTRL data. Also, all three models simulate a gradual decline from July to August. Among the three models, SWAT-GRASS_M overall better represented the seasonal dynamics of LAI, specifically in spring and early summer. This is likely a reason explaining the overall better performance of SWAT-GRASS_M.

3.4. Assessment of model simulated root to shoot ratio

Fig. 7 compares the simulated RSR across all sites for October. As described in Appendix A, SWAT calculates RSR as a function of potential heat unit (PHU), which resulted in a nearly constant RSR (0.66–0.67) at harvest. In contrast, SWAT– $GRASS_D$ and SWAT– $GRASS_M$ simulated RSR with much higher variability, ranging from 0.55 to 0.90 and 0.62 to 1.05, respectively. The high RSR variability in SWAT– $GRASS_D$ and SWAT– $GRASS_M$ results from the impacts of temperature, water, and nutrient on the biomass allocation between root and shoot, which

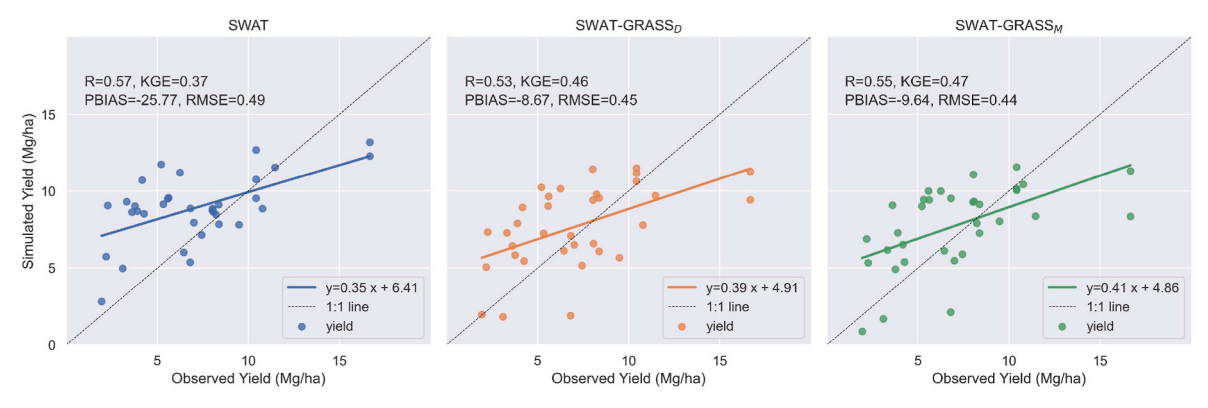


Fig. 4. SWAT, SWAT-GRASS_D, and SWAT-GRASS_M simulated annual dry weight biomass yield for all validation sites.

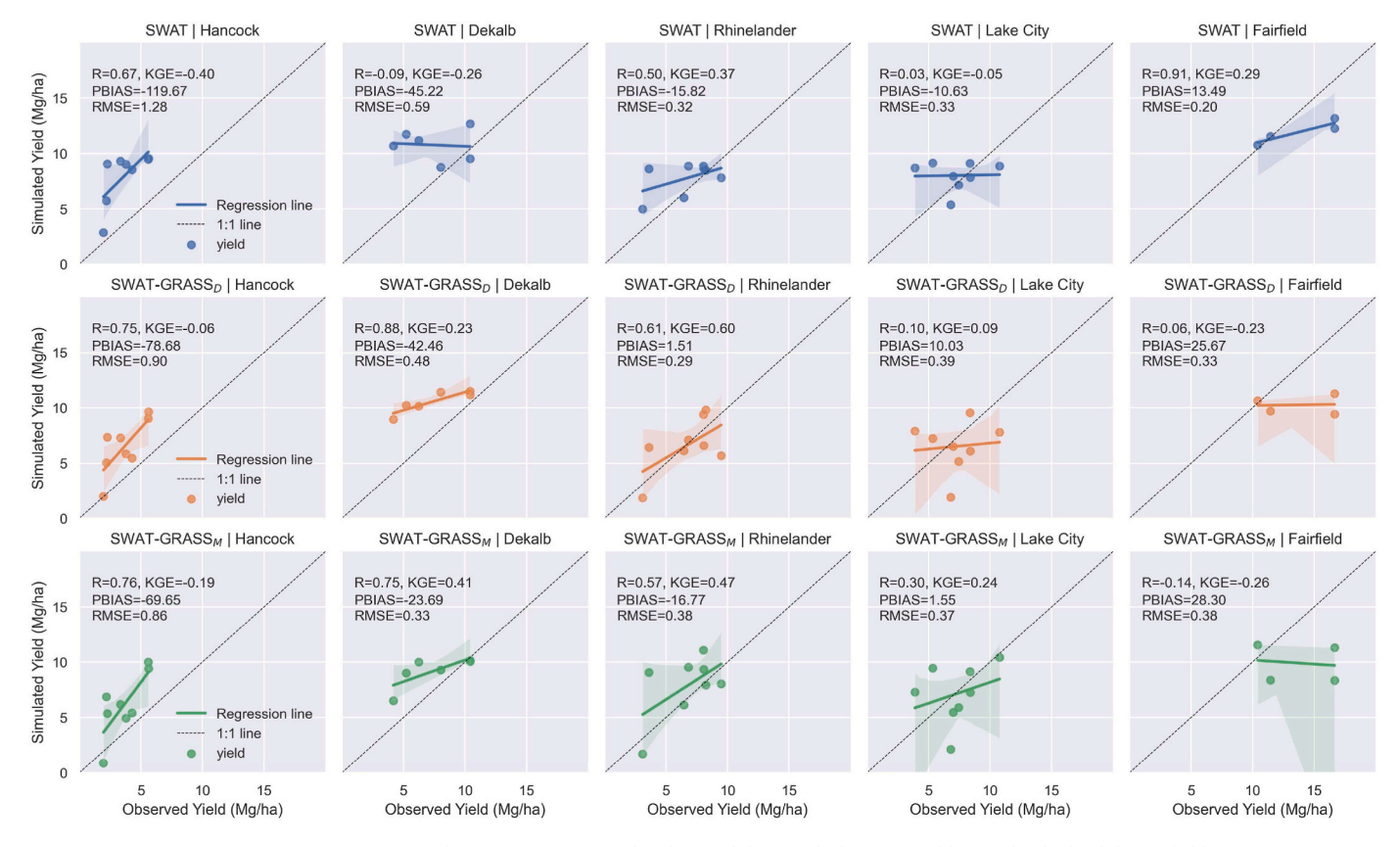


Fig. 5. SWAT, SWAT–GRASS_D, and SWAT–GRASS_M simulated annual dry weight biomass yield for individual validation field sites.

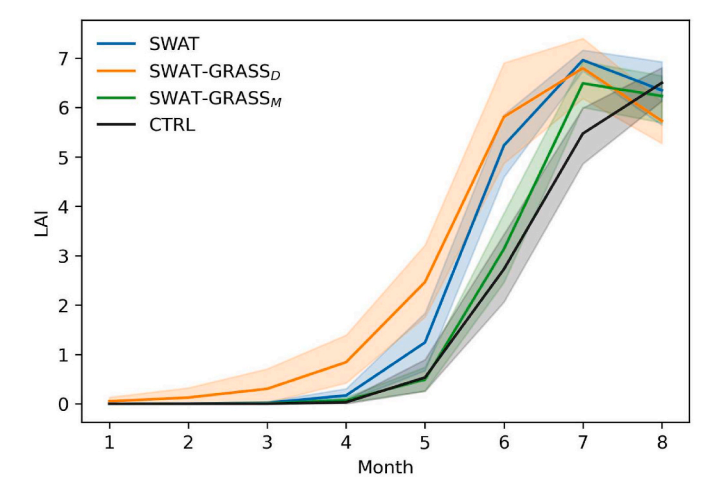


Fig. 6. Comparison of SWAT, SWAT–GRASS $_{\rm D}$, and SWAT–GRASS $_{\rm M}$ simulated LAI with regression model fitted LAI (Madakadze et al., 1998), where shading represents 95% confidence limits.

differed among the sites. In general, SWAT– $GRASS_D$ and SWAT– $GRASS_M$ allocate a high proportion of biomass to roots in warmer and wetter locations (i.e., AR sites). Specifically, the *RSR* value is high for Fairfield, Orr, and Dekalb, which receive high annual precipitation (>934 mm).

The *RSR* values fall well within the broad range of values (0.19–3.07) reported in previous observation-based studies (Frank et al., 2004; Jung and Lal, 2011; Sainju et al., 2017; Wayman et al., 2014; Zan et al., 2001). The *RSR* simulated with the three models in this study is somewhat similar to the *RSR* reported by Wayman et al. (2014), 0.88–0.95, in Nebraska and Pennsylvania where mean annual precipitation ranged between 700 and 1120 mm, and by Zan et al. (2001), which reported

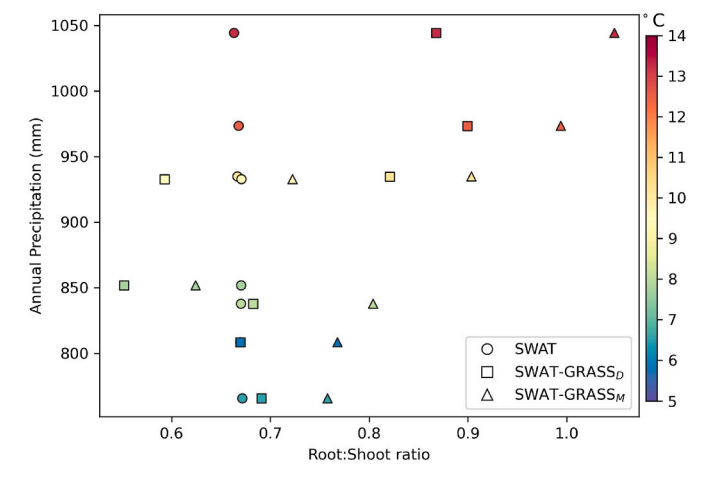


Fig. 7. Comparison of SWAT, SWAT–GRASS_D, and SWAT–GRASS_M simulated site averaged mean root-to-shoot ratio (RSR) for October. The color gradient represents the average annual temperature for each site.

RSR in the lower range of 0.4–0.7 in Quebec, Canada, with a mean air temperature of 6.5 °C and an annual precipitation of 1062 mm. It is also worth noting that other studies reported contrary findings. For example, Jung and Lal (2011), reported the RSR of 0.19–0.56 in Ohio which is smaller than the RSR estimated in this study. Sainju et al. (2017) reported high RSR in the range of 1.39–3.07 in Montana, which received low annual precipitation of 271–453 mm. These findings highlight that the variability of biomass allocation is not only influenced by climate conditions but also by nutrient and water management. Nonetheless, the observed RSR values are highly variable, therefore the constant RSR simulated by SWAT is not realistic. The observational data also

corroborate that both $SWAT-GRASS_D$ and $SWAT-GRASS_M$ can represent the effects of climate on root and shoot development.

3.5. Assessment of model simulated hydrological process and nitrogen cycle

We evaluated the impact of the differences in biomass production and LAI development as simulated by SWAT, SWAT–GRASS $_{\rm D}$, and SWAT–GRASS $_{\rm M}$ on both hydrological processes and the nitrogen cycle. In general, the seasonal cycle of surface runoff, evapotranspiration, soil moisture content, and groundwater percolation simulated by SWAT, SWAT–GRASS $_{\rm D}$, and SWAT–GRASS $_{\rm M}$ were similar (SI Figure S5), with small variations arising from the differences in biomass production and LAI development (Fig. 6). In contrast, we found substantial differences in the seasonal plant nitrogen uptake and total soil nitrate content simulated by the models, particularly during the early growing season (SI Figure S6). SWAT and SWAT–GRASS $_{\rm D}$ simulated high plant nitrogen uptake during the early growing season (Figure S6a) as reflected by the early LAI development (Fig. 6). Meanwhile, SWAT–GRASS $_{\rm M}$ exhibited lower nitrogen uptake during this period, leading to an increase in soil nitrate content (Figure S6b).

3.6. Strengths, limitations, and future directions of the SWAT-GRASS model

This study integrated and modified the DAYCENT grass sub-model into SWAT to improve the representation of biomass production, biomass allocation, and nutrient content of perennial grasses, using switchgrass as an example. SWAT considers climate conditions and nutrient availability in biomass production but does not fully account for their influence on root and shoot biomass allocation. While SWAT can satisfactorily simulate the biomass yield, it fails to simulate the high variability observed in root biomass allocation under different climatic conditions. This limits SWAT's ability to provide a credible understanding of the complex interactions between climate conditions, bioenergy feedstock production, and soil biogeochemistry. The SWAT-GRASS_D, which incorporates the DAYCENT grass sub-model into SWAT, addresses this limitation but falls short in certain aspects. For example, SWAT-GRASS_D does not explicitly account for the influence of canopy leaf area on the interception of incident solar radiation and biomass production, resulting in early plant growth and overestimation of biomass allocation and LAI in the early growing season. The introduction of an additional scaling factor that incorporates the influence of LAI dynamics in the SWAT-GRASS_M provides an improved estimation of biomass yield and LAI development.

Although none of the three models examined here can consistently outperform the others in terms of all metrics, the results show that the overall performance of SWAT– $GRASS_M$ is comparable to or better than SWAT and SWAT– $GRASS_D$ in simulating switchgrass biomass yield, in terms of R, KGE, and PBIAS for most cases. The improved performance of SWAT– $GRASS_M$ in investigating the suitability of perennial grass such as switchgrass for biomass production, which in conjunction with other capabilities within SWAT (e.g., water quantity and quality) (Arnold et al., 1998; Neitsch et al., 2011) and SWAT-Carbon (e.g., soil organic carbon and riverine carbon fluxes) (Liang et al., 2022; Qi et al., 2020; Zhang, 2018) makes it a powerful tool to study environmental impacts of using perennial grasses at the regional scale.

Note that, despite the more comprehensive algorithms in the two SWAT–GRASS models that can better represent the aboveground and belowground biomass development as influenced by climate, nutrients, and water, multiple aspects of the new models could be further improved, such as the representation of processes related to the interception of solar radiation, and the development of roots in the soil column. The current model assumes the root depth of the perennial plant to be equal to 3 m or to span the entire depth of the soil column for the entire growing period. The root depth and distribution could affect plant

water and nutrient uptake, as well as the distribution of soil organic matter. In addition, unlike SWAT, the two SWAT–GRASS models do not consider the influence of vapor pressure deficit on radiation use efficiency and subsequently impact biomass production. Therefore, further work is deserved to improve these processes in SWAT–GRASS to better simulate plant growth and biomass production of perennial grass.

Additionally, several parameters used by the two SWAT-GRASS models, such as the fraction of nutrients allocated to the root during the late growing season, vary at different ages of perennial plants. The current modification assumes that these parameters remain static throughout the lifespan of the plant. This approach could result in uncertainties regarding the model's ability to simulate nutrient uptake from soil and nutrient allocation to different plant parts. Also, comprehensive data to evaluate the model capability of representing the development of LAI, aboveground biomass, and belowground biomass were rarely available. Therefore, more comprehensive model assessment awaits future research.

Collectively, the integration and modification of the new grass submodel, which accounts for water, temperature, and nutrient stress on biomass production and allocation to plant shoot and roots, can provide reasonable (i.e. similar or better) simulation of biomass yield compared to SWAT. Particularly the SWAT–GRASS_M holds promise in simulating LAI and root and shoot development under diverse climate and management conditions more realistically. These new capabilities make it a promising tool to support future studies that examine the potential of switchgrass and other perennial grasses for biomass production and their subsequent environmental impacts and benefits. We share the new model https://sites.google.com/view/swat-carbon to facilitate future efforts to apply and further enhance the model developed in this study.

4. Conclusion

We integrated and modified the DAYCENT grass growth module into the SWAT model to improve the simulation of biomass production for perennial grasses, using switchgrass as a test example. In addition to using the default algorithms in DAYCENT (SWAT–GRASS_D), we also revised the calculation of potential biomass production (SWAT–GRASS_M) to incorporate the effect of LAI dynamics. Overall, the model improvement includes four major aspects: (1) process-based biomass allocation to root and shoot that accounts for the influence of the nutrient and water stress, such that more biomass is allocated to the root with an increase in stress; (2) process-based algorithms for plant nutrient demand and uptake during the growing period, and nutrient translocation during senescence; (3) biomass loss as surface litter/residue to the soil during plant growth and senescence; (4) scaling of potential biomass production by LAI to represent the seasonal changes in the interception of solar radiation by the plant.

All three models (i.e., SWAT, SWAT-GRASS_D, and SWAT-GRASS_M) were evaluated at eight field sites (with diverse climatic conditions) in Wisconsin, Michigan, and Illinois for biomass yield simulation. Both SWAT-GRASS_D and SWAT-GRASS_M satisfactorily simulated observed yields, and their performance metrics were comparable to or better than those of SWAT at the evaluation sites. Particularly, SWAT-GRASSD and SWAT-GRASS_M can explicitly simulate root and shoot growth as influenced by climate, nutrient, and water conditions, thereby providing more realistic estimation of the allocation of accumulated biomass and nutrients between aboveground and belowground biomass pools. This feature is critical for reliable estimates of the role of root in nutrient and carbon cycling. Notably, SWAT-GRASS_M in general outperformed SWAT-GRASS_D in terms of both biomass yield and seasonal LAI development. Overall, incorporating DAYCENT's grass module into SWAT added important capabilities to the model for credible assessment of agronomic and environmental impacts of growing perennial grasses for biomass production. The new integrated SWAT-GRASS_M model is a public domain model to support future efforts in sustainable bioenergy production.

Declaration of competing interest

The authors declare that they have no known competing financial interests or personal relationships that could have appeared to influence the work reported in this paper.

Data availability

Data will be made available on request.

Acknowledgements

We appreciate the anonymous reviewers' valuable comments which helped further improve the quality of the paper. The authors thank Dr. Evan H. DeLucia (University of Illinois at Urbana-Champaign, Urbana, IL, USA) for providing Upland switchgrass growth parameters used by the DAYCENT sub-model. The research was supported by the National Science Foundation's Innovations at the nexus of Food, Energy and Water Systems (INFEWS) under the grant EAR-1639327 and National Research Traineeship Program NRT-INFEWS under the grant 1828910, and the U.S. Department of Agriculture's National Institute of Food and Agriculture for the creation of a predictive decision support Dashboard for Agricultural Water use and Nutrient management (DAWN) under the grant 20206801231674. Dr. Zhang was supported by NASA Carbon Monitoring System (22-CMS22-0027). The research was also partially supported by the U.S. Department of Agriculture's Agricultural Research Service. Mention of supporting agency names in this publication is solely for the purpose of providing specific information and does not imply recommendation or endorsement by the funding agencies.

Appendix C. Supplementary data

Supplementary data to this article can be found online at https://doi.org/10.1016/j.envsoft.2023.105834.

Appendix A. The SWAT model's grass growth processes

A.1 Biomass allocation

The SWAT vegetation growth sub-model simulates biomass production of the entire plant as a single entity and utilizes empirical relationships to partition above and belowground biomass using the parameter plant root fraction (*RF*). The temporal evolution of *RF* is calculated in SWAT as a function of potential heat unit accumulation (PHU) and user-defined plant-specific root fraction at the planting (*rsr1*) and maturity (*rsr2*) of the growing season of plant growth (Neitsch et al., 2011).

$$RF = rsr_1 - (rsr_1 - rsr_2) \times PHU \tag{A.1}$$

The plant root fraction is then used to calculate the aboveground biomass as

above ground biomass =
$$(1 - RF) \times total$$
 plant biomass (A.2)

A.2 Plant growth constraints

SWAT incorporates multiple stress factors to limit plant biomass production. SWAT calculates temperature, water, nitrogen, and phosphorus stress at a scale of 0–1 (0 representing the maximum stress and 1 indicating no stress) (Neitsch et al., 2011). The most limiting factor among the four plant stress is then used to adjust the potential biomass production.

$$Stress_{T} = \begin{cases} 1 & when T_{avg} \leq T_{base} \\ 1 - exp \left[\frac{-0.1054 \left(T_{opt} - T_{avg} \right)^{2}}{\left(T_{avg} - T_{base} \right)^{2}} \right] & when T_{base} \leq T_{avg} \leq T_{opt} \\ 1 - exp \left[\frac{-0.1054 \left(T_{opt} - T_{avg} \right)^{2}}{\left(2T_{opt} - T_{avg} - T_{base} \right)^{2}} \right] & when T_{opt} \leq T_{avg} \leq 2T_{opt} - T_{base} \end{cases}$$
(A3)

$$Stress_W = 1 - \frac{W_{actualup}}{E_t} \tag{A.4}$$

$$Stress_E = 1 - \frac{\varphi_E}{\varphi_E + exp(3.535 - 0.2597\varphi_E)}$$
 (A.5)

$$\varphi_E = 200 \left(\frac{bio_E}{bio_{E,opt}} - 0.5 \right) \tag{A.6}$$

Where, $T_{avg}(^{\circ}C)$ is the average air temperature, $T_{opt}(^{\circ}C)$ is the optimum temperature for plant growth, T_{base} ($^{\circ}C$) is the base temperature for plant growth, $W_{actualup}$ (mm H2O/day) is the actual plant water uptake, E_t (mm H₂O/day) is the maximum plant transpiration, φ_E is the scaling factor for nutrient E = N, P (nitrogen, N and phosphorous, P), bio_E (kg E/ha) is the amount of nutrient E in plant biomass, and E (kg E/ha) is the optimal amount of nutrient E in plant biomass, and E (kg E/ha) is the optimal amount of nutrient E in plant biomass, and E (kg E/ha) is the optimal amount of nutrient E in plant biomass, and E (kg E/ha) is the optimal amount of nutrient E in plant biomass, and E (kg E/ha) is the optimal amount of nutrient E in plant biomass, and E (kg E/ha) is the optimal amount of nutrient E in plant biomass, and E (kg E/ha) is the optimal amount of nutrient E in plant biomass, and E (kg E/ha) is the optimal amount of nutrient E (not not not not not nutrient E (kg E/ha) is the optimal amount of nutrient E (not not not not nutrient E (kg E/ha) is the optimal amount of nutrient E (hg) is the optimal E (hg) is the o

A.3 Plant nutrient demand

In the SWAT model, the daily nutrient uptake by plant is calculated as a function of the difference between plant actual nutrient content and plant optimal nutrient content, and soil nutrient availability. The plant-specific parameters for nutrient fraction parameters for each nutrient (nitrogen and phosphorous) which characterizes the optimal contents of nutrients in the plant at three growth stages (emergence, 50% maturity, and maturity). Nutrient fraction parameters for nitrogen (*PLTNFR*) and phosphorus (*PLTPFR*) are defined at the three growth stages and used to calculate the plant optimal nutrient content at different stages of plant growth. Furthermore, SWAT uses two plant-specific parameters, the fraction of nitrogen (*CPNYLD*) and phosphorus (*CPPYLD*) in aboveground biomass at harvest, to calculate the amount of nutrients removed during harvest operation that subsequently affects the nutrients added to soil from harvest residue.

Appendix B. The DAYCENT model's grass growth processes

B.1 Potential biomass production

Incoming solar radiation is provided as an input to the vegetation growth sub-model for estimating the potential biomass production. The potential plant biomass production is calculated as a function of a plant-specific maximum monthly biomass production and scaled by six terms (values between 0 and 1) that represent the effects of climatic conditions and plant phenology, respectively. DAYCENT uses the multiplication of stress factors under the assumption that the interactions of multiple stress factors limit plant biomass production (Del Grosso et al., 2008).

$$tgprod = shwave \times prdx \times T_{stress} \times SM_{stress} \times Sdlng \times CO2cpr \times scenfrac \times biof$$
(B.1)

where, $tgprod (g C/m^2)$ is the potential biomass production on a given day, shwave is downwelling solar radiation (Lg/day), shsum shape solar radiation (<math>Lg/day), shsum shape shape shape solar radiation (<math>Lg/day), shsum shape shap

$$T_{stress} = \begin{cases} exp\left(\frac{ppdf(3)}{ppdf(4)} \times \left(1 - frac^{ppdf(4)}\right)\right) \times \left(frac^{ppdf(3)}\right) & \text{if } frac > 0\\ 0 & \text{if } frac \le 0 \end{cases}$$
(B.2)

$$frac = \frac{ppdf(2) - Tavg}{ppdf(2) - ppdf(1)}$$
(B.3)

where, Tavg is the average air temperature (°C), ppdf(1) is the minimum temperature for plant growth (°C), ppdf(2) is the optimum temperature for plant growth (°C), ppdf(3) is the left shape coefficient of the function curve of temperature effect on growth, and ppdf(4) is the right shape coefficient of the function curve of temperature effect on growth

$$SM_{stress} = \begin{cases} \frac{1.0}{(1.0 + \exp(9.0 * (wscoeff(1) - cwstress)))} & \text{if PET} \ge 0.01\\ 0.01 & \text{if PET} < 0.01 \end{cases}$$
(B.4)

where, wscoeff(1) (unitless) is the relative water content required for 50% of maximum production and cwstress (unitless) is the relative water content of the wettest soil layer.

$$cwstres = max \left(\frac{SWC_l - WP_l}{FC_l - WP_l} \right)$$
(B.5)

where, SWC_b , WP_b , and FC_l are, respectively, the soil water content (cm H_2O), soil water content at wilting point (cm H_2O), and soil water content at field capacity (cm H_2O) of soil layer l.

$$CO2cpr = 1 + \frac{(co2ipr - 1)}{\log 10(2.0)} l \times \log 10 \left(\frac{co2}{330}\right)$$
(B.6)

where, co2ipr (unitless) is the plant production ratio when atmospheric CO2 concentration is doubled, co2 is atmospheric CO2 concentration (ppmv).

$$Sdlng = \begin{cases} MIN\left(1.0, pltmrf + aglivc \times \frac{(1 - pltmrf)}{fulcan}\right) & when PHU < 0.25\\ 1 & when PHU \ge 0.25 \end{cases}$$
(B.7)

where, *pltmrf* (unitless) is the reduction factor to limit the seedling growth, *aglivc* is aboveground live carbon ($g C/m^2$), and *fulcan* is aboveground live carbon full canopy cover ($g C/m^2$)

$$biof = \begin{cases} bioprd + 0.75 \times (1 - bioprd) \times \frac{aglivc}{bioc} & if \frac{aglivc}{bioc} \le 1 \\ bioprd + 0.75 \times (1 - bioprd) + 0.25 \times (1 - bioprd) \times \left(\frac{aglivc}{bioc} - 1\right) & if 1 < \frac{aglivc}{bioc} \le 2 \\ biof = 1 & if \frac{aglivc}{bioc} > 2 \end{cases}$$
(B.8)

$$bioprd = 1 - \frac{bioc}{biok5 + bioc} \tag{B.9}$$

$$bioc = \begin{cases} stdcis + 0.1 \times sol_{rsd(surface)} \\ 0.1 \quad \text{if } stdcis + 0.1 \times sol_{rsd(surface)} \le 0 \\ pmxbio \quad \text{if } stdcis + 0.1 \times sol_{rsd(surface)} > pmxbio \end{cases}$$
(B.10)

where, biok5 is (standing dead+10% surface litter) carbon at which production is reduced to half maximum due to physical obstruction by dead material (gC/m^2), pmxbio is the maximum standing dead biomass +10% surface litter carbon for calculation of the potential negative effect of physical obstruction by standing dead and surface litter on biomass production (gC/m^2), stdcis is standing dead carbon (gC/m^2), sol_{rsd} (surface) is plant residue carbon in surface soil layer (gC/m^2). For compatibility with SWAT, biomass production ceases when the accumulated potential heat unit exceeds 1 (i. e. plant maturity).

B.2 Actual biomass production and allocation

The plant-specific parameters are used to estimate the RF (unitless) to allocate the potential biomass production to the different plant compartments (aboveground and belowground). The optimum RF is calculated as a function of four plant-specific parameters (cfrtcn(1), cfrtcn(2), cfrtcw(1), cfrtcw(2)), that represents the maximum and minimum fraction of carbon allocated to root under nutrient and water stress.

$$RF = (cfrtcw(1) + cfrtcw(2) + cfrtcn(1) + cfrtcn(2))/4.0$$
(B.11)

The calculated optimum *RF* is then used to partition the potential plant biomass into aboveground and belowground components. In addition, the optimum *RF* is used to compute the plant nutrient demand taking into account the impact of root biomass (*rtimp*) on the availability of nutrients from the soil.

The nutrient uptake by the aboveground and belowground biomass is dependent on the availability of nutrients and nutrient content of the plant which is further constrained between plant-specific upper and lower nutrient limits set for both plant compartments. To adjust for changes in nutrient content as the plant ages, the limits of the nutrient content of aboveground biomass are calculated as a function of aboveground biomass. Meanwhile, the limits of the nutrient content of belowground biomass are calculated as a function of annual precipitation. The most limiting nutrient is then used to scale the potential biomass production and calculate the actual biomass production and corresponding nutrient concentration and nutrient uptake. A linear relationship is then used to estimate the impact of water and nutrient limitations on the allocation of actual biomass between shoot and root. The water limitation is calculated as a function of soil moisture effect on potential production and plant-specific parameter *cftrcw*. The nutrient limitation is calculated as a function of nutrient stress and plant-specific parameter *cftrcn*. The most limiting factor between the water and nutrient limitation is used to determine the actual fraction of biomass allocated to the root. This approach incorporates the plant's response to water and nutrient stress such that more allocation of biomass to the root takes place when water and nutrient stress increases.

$$fract = max(h2oeff, ntreff(iel))$$
 (B.12)

$$h2oeff = (cftrcw(2) - cftrcw(1)) \times (SM_{stress} - 1) + cfrtcw(2)$$
(B.13)

$$\textit{ntreff}(\textit{iel}) = (\textit{cftrcn}(2) - \textit{cftrcn}(1)) \times \left(\frac{\textit{totale}(\textit{iel})}{\textit{demand}(\textit{iel})} - 1\right) + \textit{cfrtcn}(2) \tag{B.14}$$

where, *iel* represents nutrients nitrogen or phosphorous, *totale(iel)* is the nutrient *iel* (nitrogen or phosphorous) available for biomass production ($g E/m^2$), and *demand(iel)* is plant demand of nutrient *iel* for optimum biomass production ($g E/m^2$).

The potential aboveground and belowground biomass is then calculated as

$$bgprod = tgprod * fracrc$$
 (B.15)

$$agprod = tgprod - bgprod$$
 (B.16)

where, tgprod is total plant biomass (g/m^2) , agprod is aboveground biomass (g/m^2) , and bgprod is belowground biomass (g/m^2) . The belowground biomass is further categorized into juvenile and mature roots.

B.3 Shoot and root die-off

Unlike SWAT, the death of shoot and root is simulated in the growing season. The shoot and root death are determined by soil moisture, soil temperature, and plant-specific maximum senescence parameters. Root death takes place when the soil temperature is greater than 2° C. In senescence months (i.e., when PHU > Fraction of growing season when leaf area starts declining, DLAI) shoot death rate is set to a fixed plant-specific fraction *fsdeth(2)*. The dead shoot biomass (standing dead) is transferred to the surface soil layer (0–10 cm) as the plant residue at the plant-specific fall rate (*fallrt*). Meanwhile, the dead root biomass is distributed to different soil layers based on the depth distribution of roots in the soil column following the

approach used by SWAT during plant kill operations. During dormancy, SWAT assumes 10% of plant biomass is returned to the surface soil layer as plant residue, which is adopted in the new sub-model.

B.4 Plant nutrient storage

The DAYCENT grass sub-model simulates the nutrient flow for the nutrient storage pool in addition to the nutrient flow for each plant compartment. A fraction of nutrients from aboveground biomass which is converted to standing dead material is transferred to the nutrient storage pool during the growing season. In addition, a fraction of nutrient uptake by the plant from the soil during the late growing season is allocated to the nutrient storage pool. The nutrients accumulated in the storage pool are remobilized by the plant during the early growth phase such that plants use nutrients in the storage pool before utilizing soil nutrients for biomass production.

Nutrient uptake from the internal plant storage pool by each plant compartment is calculated as

$$uptake_{above} = \begin{cases} uptake_{storage,iel} \times euf_{above} \times (1.0 - clsgres) & if PHU > 0.8 \\ uptake_{storage,iel} \times euf_{above} & if PHU \le 0.8 \end{cases}$$
(B.17)

$$uptake_{below} = uptake_{storage,iel} \times euf_{below}$$
 (B.18)

Nutrient flow into the internal plant storage pool is calculated as.

Step 1. Obtained from the conversion of aboveground live biomass to standing dead

$$storage(iel) = fdeth \times aglive(iel) \times crprtf(iel)$$
 (B.19)

Step 2. Obtained from soil nutrient uptake during the late growing season

$$storage(iel) = uptake_{soil.iel} \times euf_{above} \times clsgres \quad if \ PHU > 0.8$$
 (B.20)

where, $uptake_{soil,iel}$ is the plant uptake of nutrient iel from soil (g E/m²), $uptake_{storage,iel}$ is plant uptake of nutrient iel from the internal storage pool (g E/m²), fdeth is the death rate of shoots to standing dead, aglive(iel) is the concentration of nutrient iel in the plant (g E/m²), clsgres is late growing season restriction factor (0–1), crprtf(iel) is the fraction of nutrient iel translocated from aboveground biomass at death, euf_{above} is the fraction of nutrient uptake from aboveground biomass, and euf_{below} is the fraction of nutrient uptake from belowground biomass.

References

- Abbaspour, K.C., Rouholahnejad, E., Vaghefi, S., Srinivasan, R., Yang, H., Kløve, B., 2015. A continental-scale hydrology and water quality model for Europe: calibration and uncertainty of a high-resolution large-scale SWAT model. J. Hydrol. 524, 733–752.
- Agostini, F., Gregory, A.S., Richter, G.M., 2015. Carbon sequestration by perennial energy crops: is the jury still out? Bioenerg. Res. 8, 1057–1080. https://doi.org/ 10.1007/s12155-014-9571-0.
- Anderson-Teixeira, K.J., Davis, S.C., Masters, M.D., Delucia, E.H., 2009. Changes in soil organic carbon under biofuel crops. GCB Bioenergy 1, 75–96. https://doi.org/10.1111/j.1757-1707.2008.01001.x.
- Arnold, J.G., Srinivasan, R., Muttiah, R.S., Williams, J.R., 1998. Large area hydrologic modeling and assessment part I: model development 1. JAWRA Journal of the American Water Resources Association 34, 73–89. https://doi.org/10.1111/j.1752-1688.1998.tb05961.x.
- Arundale, R.A., Dohleman, F.G., Heaton, E.A., Mcgrath, J.M., Voigt, T.B., Long, S.P., 2014. Yields of *Miscanthus* × *giganteus* and *Panicum virgatum* decline with stand age in the Midwestern USA. GCB Bioenergy 6, 1–13. https://doi.org/10.1111/gcbb.12077.
- Ashworth, A.J., Allen, F.L., Bacon, J.L., Sams, C.E., Hart, W.E., Grant, J.F., Moore, P.A., Pote, D.H., 2017. Switchgrass cultivar, yield, and nutrient removal responses to harvest timing. Agron. J. 109, 2598–2605. https://doi.org/10.2134/ agronj2017.01.0018
- Chamberlain, J.F., Miller, S.A., Frederick, J.R., 2011. Using DAYCENT to quantify onfarm GHG emissions and N dynamics of land use conversion to N-managed switchgrass in the Southern U.S. Agriculture. Ecosystems & Environment 141, 332–341. https://doi.org/10.1016/j.agee.2011.03.011.
- 332–341. https://doi.org/10.1016/j.agee.2011.03.011.
 Chen, L., Blanc-Betes, E., Hudiburg, T.W., Hellerstein, D., Wallander, S., DeLucia, E.H., Khanna, M., 2021. Assessing the returns to land and greenhouse gas savings from producing energy crops on conservation reserve Program land. Environ. Sci. Technol. 55, 1301–1309. https://doi.org/10.1021/acs.est.0c06133.
- Cibin, R., Trybula, E., Chaubey, I., Brouder, S.M., Volenec, J.J., 2016. Watershed-scale impacts of bioenergy crops on hydrology and water quality using improved SWAT model. GCB Bioenergy 8, 837–848. https://doi.org/10.1111/gcbb.12307.
- Clifton-Brown, J., Harfouche, A., Casler, M.D., Dylan Jones, H., Macalpine, W.J., Murphy-Bokern, D., Smart, L.B., Adler, A., Ashman, C., Awty-Carroll, D., Bastien, C., Bopper, S., Botnari, V., Brancourt-Hulmel, M., Chen, Z., Clark, L.V., Cosentino, S., Dalton, S., Davey, C., Dolstra, O., Donnison, I., Flavell, R., Greef, J., Hanley, S., Hastings, A., Hertzberg, M., Hsu, T., Huang, L.S., Iurato, A., Jensen, E., Jin, X., Jørgensen, U., Kiesel, A., Kim, D., Liu, J., McCalmont, J.P., McMahon, B.G., Mos, M., Robson, P., Sacks, E.J., Sandu, A., Scalici, G., Schwarz, K., Scordia, D., Shaffei, R., Shield, I., Slavov, G., Stanton, B.J., Swaminathan, K., Taylor, G., Torres, A.F., Trindade, L.M., Tschaplinski, T., Tuskan, G.A., Yamada, T., Yeon Yu, C., Zalesny, R.

- S., Zong, J., Lewandowski, I., 2019. Breeding progress and preparedness for mass-scale deployment of perennial lignocellulosic biomass crops switchgrass, miscanthus, willow and poplar. GCB Bioenergy 11, 118–151. https://doi.org/10.1111/gcbb.12566.
- Clifton-Brown, J.C., Breuer, J., Jones, M.B., 2007. Carbon mitigation by the energy crop, Miscanthus. Global Change Biol. 13, 2296–2307. https://doi.org/10.1111/j.1365-
- Davis, S.C., Parton, W.J., Dohleman, F.G., Smith, C.M., Grosso, S.D., Kent, A.D., DeLucia, E.H., 2010. Comparative biogeochemical cycles of bioenergy crops reveal nitrogen-fixation and low greenhouse gas emissions in a miscanthus × giganteus agro-ecosystem. Ecosystems 13, 144–156. https://doi.org/10.1007/s10021-009-9306-9.
- Del Grosso, S.J., Parton, W.J., Ojima, D.S., Keough, C.A., Riley, T.H., Mosier, A.R., 2008. DAYCENT simulated effects of land use and climate on county level N loss vectors in the USA. In: Nitrogen in the Environment. Elsevier, pp. 571–595. https://doi.org/10.1016/B978-0-12-374347-3.00018-4.
- Egbendewe-Mondzozo, A., Swinton, S.M., Izaurralde, C.R., Manowitz, D.H., Zhang, X., 2011. Biomass supply from alternative cellulosic crops and crop residues: a spatially explicit bioeconomic modeling approach. Biomass Bioenergy 35, 4636–4647. https://doi.org/10.1016/j.biombioe.2011.09.010.
- Egbendewe-Mondzozo, A., Swinton, S.M., Izaurralde, R.C., Manowitz, D.H., Zhang, X., 2013. Maintaining environmental quality while expanding biomass production: subregional U.S. policy simulations. Energy Pol. 57, 518–531. https://doi.org/10.1016/ j.enpol.2013.02.021.
- Fernández-Martínez, M., Vicca, S., Janssens, I.A., Ciais, P., Obersteiner, M., Bartrons, M., Sardans, J., Verger, A., Canadell, J.G., Chevallier, F., Wang, X., Bernhofer, C., Curtis, P.S., Gianelle, D., Grünwald, T., Heinesch, B., Ibrom, A., Knohl, A., Laurila, T., Law, B.E., Limousin, J.M., Longdoz, B., Loustau, D., Mammarella, I., Matteucci, G., Monson, R.K., Montagnani, L., Moors, E.J., Munger, J.W., Papale, D., Piao, S.L., Peñuelas, J., 2017. Atmospheric deposition, CO2, and change in the land carbon sink. Sci. Rep. 7, 9632. https://doi.org/10.1038/s41598-017-08755-8.
- Frank, A.B., Berdahl, J.D., Hanson, J.D., Liebig, M.A., Johnson, H.A., 2004. Biomass and carbon partitioning in switchgrass. Crop Sci. 44, 1391–1396. https://doi.org/ 10.2135/cropsci2004.1391.
- Gassman, P.W., Arnold, J.J., Srinivasan, R., Reyes, M., 2010. The worldwide use of the SWAT model: technological drivers, networking impacts, and simulation trends. In: 21st Century Watershed Technology: Improving Water Quality and Environment Conference Proceedings, 21-24 February 2010, Universidad EARTH, Costa Rica. Presented at the 21st Century Watershed Technology: Improving Water Quality and Environment Conference Proceedings, vols. 21–24. Universidad EARTH, Costa Rica, American Society of Agricultural and Biological Engineers. https://doi.org/ 10.13031/2013.29418. February 2010.

- Gelfand, I., Sahajpal, R., Zhang, X., Izaurralde, R.C., Gross, K.L., Robertson, G.P., 2013. Sustainable bioenergy production from marginal lands in the US Midwest. Nature 493, 514–517. https://doi.org/10.1038/nature11811.
- Gopalakrishnan, G., Cristina Negri, M., Salas, W., 2012. Modeling biogeochemical impacts of bioenergy buffers with perennial grasses for a row-crop field in Illinois. Glob. Change Biol. Bioenergy 4, 739–750. https://doi.org/10.1111/j.1757-1707.2011.01145.x
- Gupta, H.V., Kling, H., Yilmaz, K.K., Martinez, G.F., 2009. Decomposition of the mean squared error and NSE performance criteria: implications for improving hydrological modelling. J. Hydrol. 377, 80–91. https://doi.org/10.1016/j.jhydrol.2009.08.003.
- Hartman, J.C., Nippert, J.B., Springer, C.J., 2012. Ecotypic responses of switchgrass to altered precipitation. Funct. Plant Biol. 39, 126. https://doi.org/10.1071/FP11229.
- He, Y., Jaiswal, D., Liang, X., Sun, C., Long, S.P., 2022. Perennial biomass crops on marginal land improve both regional climate and agricultural productivity. GCB Bioenergy 14, 558–571. https://doi.org/10.1111/gcbb.12937.
- Hudiburg, T.W., Davis, S.C., Parton, W., Delucia, E.H., 2015. Bioenergy crop greenhouse gas mitigation potential under a range of management practices. GCB Bioenergy 7, 366–374. https://doi.org/10.1111/gcbb.12152.
- Hudiburg, T.W., Wang, W., Khanna, M., Long, S.P., Dwivedi, P., Parton, W.J., Hartman, M., Delucia, E.H., 2016. Impacts of a 32-billion-gallon bioenergy landscape on land and fossil fuel use in the US. Nat. Energy 1, 15005. https://doi. org/10.1038/nenergy.2015.5.
- Jarvis, A., Reuter, H.I., Nelson, A., Guevara, E., 2008. Hole-filled SRTM for the globe Version 4. available from the CGIAR-CSI SRTM 90m Database 15, 25–54. http:// srtm.csi.cgiar.org.
- Jung, J.Y., Lal, R., 2011. Impacts of nitrogen fertilization on biomass production of switchgrass (Panicum Virgatum L.) and changes in soil organic carbon in Ohio. Geoderma 166, 145–152. https://doi.org/10.1016/j.geoderma.2011.07.023.
- Kantola, I.B., Masters, M.D., Blanc-Betes, E., Gomez-Casanovas, N., DeLucia, E.H., 2022. Long-term yields in annual and perennial bioenergy crops in the Midwestern United States. GCB Bioenergy 14, 694–706. https://doi.org/10.1111/gcbb.12940.
- Kiniry, J.R., Schmer, M.R., Vogel, K.P., Mitchell, R.B., 2008. Switchgrass biomass simulation at diverse sites in the northern great plains of the. U.S. Bioenerg. Res. 1, 259–264. https://doi.org/10.1007/s12155-008-9024-8.
- Lark, T.J., Hendricks, N.P., Smith, A., Pates, N., Spawn-Lee, S.A., Bougie, M., Booth, E.G., Kucharik, C.J., Gibbs, H.K., 2022. Environmental outcomes of the US renewable fuel standard. Proc. Natl. Acad. Sci. U.S.A. 119, e2101084119 https://doi.org/10.1073/pnas.2101084119.
- Larnaudie, V., Ferrari, M.D., Lareo, C., 2022. Switchgrass as an alternative biomass for ethanol production in a biorefinery: perspectives on technology, economics and environmental sustainability. Renew. Sustain. Energy Rev. 158, 112115 https://doi. org/10.1016/j.rser.2022.112115.
- LeDuc, S.D., Zhang, X., Clark, C.M., Izaurralde, R.C., 2017. Cellulosic feedstock production on Conservation Reserve Program land: potential yields and environmental effects. GCB Bioenergy 9, 460–468. https://doi.org/10.1111/ gcbb.12352.
- Lee, J., Pedroso, G., Linquist, B.A., Putnam, D., Kessel, C., Six, J., 2012. Simulating switchgrass biomass production across ecoregions using the DAYCENT model. Glob. Change Biol. Bioenergy 4, 521–533. https://doi.org/10.1111/j.1757-1707 2011 01140 x
- Li, X., Petipas, R.H., Antoch, A.A., Liu, Y., Stel, H.V., Bell-Dereske, L., Smercina, D.N., Bekkering, C., Evans, S.E., Tiemann, L.K., Friesen, M.L., 2022. Switchgrass cropping systems affect soil carbon and nitrogen and microbial diversity and activity on marginal lands. GCB Bioenergy 14, 918–940. https://doi.org/10.1111/gcbb.12949.
- Liang, K., Qi, J., Zhang, X., Deng, J., 2022. Replicating measured site-scale soil organic carbon dynamics in the U.S. Corn Belt using the SWAT-C model. Environ. Model. Software 158, 105553. https://doi.org/10.1016/j.envsoft.2022.105553.
- Luo, Y., He, C., Sophocleous, M., Yin, Z., Hongrui, R., Ouyang, Z., 2008. Assessment of crop growth and soil water modules in SWAT2000 using extensive field experiment data in an irrigation district of the Yellow River Basin. J. Hydrol. 352, 139–156. https://doi.org/10.1016/j.jhydrol.2008.01.003.
- Madakadze, I.C., Coulman, B.E., Peterson, P., Stewart, K.A., Samson, R., Smith, D.L., 1998. Leaf area development, light interception, and yield among switchgrass populations in a short-season area. Crop Sci. 38, 827–834. https://doi.org/10.2135/ cropsci1998.0011183X003800030035x.
- Martinez-Feria, R., Basso, B., 2020. Predicting soil carbon changes in switchgrass grown on marginal lands under climate change and adaptation strategies. GCB Bioenergy 12, 742–755. https://doi.org/10.1111/gcbb.12726.
- Massey, J., Antonangelo, J., Zhang, H., 2020. Nutrient dynamics in switchgrass as a function of time. Agronomy 10, 940. https://doi.org/10.3390/agronomy1007094
- Mehmood, M.A., Ibrahim, M., Rashid, U., Nawaz, M., Ali, S., Hussain, A., Gull, M., 2017. Biomass production for bioenergy using marginal lands. Sustain. Prod. Consum. 9, 3–21. https://doi.org/10.1016/j.spc.2016.08.003.
 Metherell, A.K., Harding, L.A., Cole, C.V., Parton, W.J., 1993. CENTURY Soil Organic
- Metherell, A.K., Harding, L.A., Cole, C.V., Parton, W.J., 1993. CENTURY Soil Organic Matter Model Environment. Great Plains System Research Unit, USDA-ARS, Fort Collins, Colorado, USA. Technical documentation. Agroecosystem version 4.0. (Technical Report No. 4).
- Miguez, F.E., Maughan, M., Bollero, G.A., Long, S.P., 2012. Modeling spatial and dynamic variation in growth, yield, and yield stability of the bioenergy crops Miscanthus × giganteus and Panicum virgatum across the conterminous United States. Glob. Change Biol. Bioenergy 4, 509–520. https://doi.org/10.1111/j.1757-1707.2011.01150.x.
- Moriasi, D.N., Arnold, J.G., Van Liew, M.W., Bingner, R.L., Harmel, R.D., Veith, T.L., 2007. Model evaluation guidelines for systematic quantification of accuracy in watershed simulations. Transactions of the ASABE 50, 885–900.

- NADP, 2022. National Atmospheric Deposition Program (NRSP-3). NADP Program Office, Wisconsin State Laboratory of Hygiene, 465 Henry Mall, Madison, WI 53706. National Research Council, 2009. Liquid Transportation Fuels from Coal and Biomass:
- National Research Council, 2009. Liquid Transportation Fuels from Coal and Biomass: Technological Status, Costs, and Environmental Impacts. National Academies Press, Washington. D.C.
- Neitsch, S.L., Arnold, J.G., Kiniry, J.R., Williams, J.R., 2011. Soil and Water Assessment Tool Theoretical Documentation Version 2009. Texas Water Resources Institute
- Nelson, R.G., Ascough, J.C., Langemeier, M.R., 2006. Environmental and economic analysis of switchgrass production for water quality improvement in northeast Kansas. J. Environ. Manag. 79, 336–347. https://doi.org/10.1016/j. ienvman.2005.07.013.
- Ng, T.L., Eheart, J.W., Cai, X., Miguez, F., 2010. Modeling miscanthus in the soil and water assessment tool (SWAT) to simulate its water quality effects as a bioenergy crop. Environ. Sci. Technol. 44, 7138–7144. https://doi.org/10.1021/es9039677.
- Nocentini, A., Di Virgilio, N., Monti, A., 2015. Model simulation of cumulative carbon sequestration by switchgrass (Panicum virgatum L.) in the mediterranean area using the DAYCENT model. Bioenerg. Res. 8, 1512–1522. https://doi.org/10.1007/s12155-015-9672-4.
- Parton, W.J., Hartman, M., Ojima, D., Schimel, D., 1998. DAYCENT and its land surface submodel: description and testing. Global Planet. Change 19, 35–48. https://doi. org/10.1016/S0921-8181(98)00040-X.
- Proulx, R.A., Hill, M.J., Laguette, S., 2022. Improved ALMANAC simulations of upland switchgrass ecotypes in the northern United States. Agron. J. 114, 508–523. https:// doi.org/10.1002/agi2.20970.
- Qi, J., Du, X., Zhang, X., Lee, S., Wu, Y., Deng, J., Moglen, G.E., Sadeghi, A.M., McCarty, G.W., 2020. Modeling riverine dissolved and particulate organic carbon fluxes from two small watersheds in the northeastern United States. Environ. Model. Software 124, 104601. https://doi.org/10.1016/j.envsoft.2019.104601.
- Qin, Z., Zhuang, Q., Chen, M., 2012. Impacts of land use change due to biofuel crops on carbon balance, bioenergy production, and agricultural yield, in the conterminous United States. Glob. Change Biol. Bioenergy 4, 277–288. https://doi.org/10.1111/ j.1757-1707.2011.01129.x.
- Rasse, D.P., Rumpel, C., Dignac, M.-F., 2005. Is soil carbon mostly root carbon? Mechanisms for a specific stabilisation. Plant Soil 269, 341–356. https://doi.org/ 10.1007/s11104-004-0907-y.
- Sainju, U.M., Allen, B.L., Lenssen, A.W., Ghimire, R.P., 2017. Root biomass, root/shoot ratio, and soil water content under perennial grasses with different nitrogen rates. Field Crops Res. 210, 183–191. https://doi.org/10.1016/j.fcr.2017.05.029.
- Schnepf, R., Yacobucci, B.D., 2013. Renewable Fuel Standard (RFS): Overview and Issues (No. R40155). Congressional Research Service.
- Searchinger, T., Heimlich, R., Houghton, R.A., Dong, F., Elobeid, A., Fabiosa, J., Tokgoz, S., Hayes, D., Yu, T.-H., 2008. Use of U.S. Croplands for biofuels increases greenhouse gases through emissions from land-use change. Science 319, 1238–1240. https://doi.org/10.1126/science.1151861.
- Sharara, M.A., Sahoo, K., Reddy, A.D., Kim, S., Zhang, X., Dale, B., Jones, C.D., Izaurralde, R.C., Runge, T.M., 2020. Sustainable feedstock for bioethanol production: impact of spatial resolution on the design of a sustainable biomass supply-chain. Bioresour. Technol. 302, 122896 https://doi.org/10.1016/j. biortech.2020.122896.
- Sinistore, J.C., Reinemann, D.J., Izaurralde, R.C., Cronin, K.R., Meier, P.J., Runge, T.M., Zhang, X., 2015. Life cycle assessment of switchgrass cellulosic ethanol production in the Wisconsin and Michigan agricultural contexts. Bioenerg. Res. 8, 897–909. https://doi.org/10.1007/s12155-015-9611-4.
- Srinivasan, R., Zhang, X., Arnold, J., 2010. SWAT ungauged: hydrological budget and crop yield predictions in the upper Mississippi River basin. Transactions of the ASABE 53, 1533–1546. https://doi.org/10.13031/2013.34903.
- Sullivan, T.P., Gao, Y., 2016. Assessment of nitrogen inputs and yields in the Cibolo and Dry Comal Creek watersheds using the SWAT model, Texas, USA 1996–2010. Environ. Earth Sci. 75, 725. https://doi.org/10.1007/s12665-016-5546-0.
- Trybula, E.M., Cibin, R., Burks, J.L., Chaubey, I., Brouder, S.M., Volenec, J.J., 2015.

 Perennial rhizomatous grasses as bioenergy feedstock in SWAT: parameter development and model improvement. GCB Bioenergy 7, 1185–1202. https://doi.org/10.1111/gcbb.12210.
- U.S. EPA, 2022. Biofuels and the Environment: Third Triennial Report to Congress (External Review Draft). U.S. EPA. No. EPA/600/R-22/273.
- USDA NASS Cropland Data Layer, 2008. Published crop-specific data layer [Online].

 Available at. USDA-NASS, Washington, DC. https://nassgeodata.gmu.edu/CropScape/. accessed March 2018.
- USDA-NRCS, 1994. State Soil Geographic (STATSGO) Database Data User Guide. U.S. Department of Agriculture, Natural Resources Conservation Service, Misc. Publ. 1492, Washington, D.C.
- Wayman, S., Bowden, R.D., Mitchell, R.B., 2014. Seasonal changes in shoot and root nitrogen distribution in switchgrass (Panicum virgatum). Bioenerg. Res. 7, 243–252. https://doi.org/10.1007/s12155-013-9365-9.
- Williams, J.R., Jones, C.A., Kiniry, J.R., Spanel, D.A., 1989. The EPIC crop growth model. Transactions of the ASAE 32, 497–511. https://doi.org/10.13031/2013.31032.
- Xia, Y., Mitchell, K., Ek, M., Sheffield, J., Cosgrove, B., Wood, E., Luo, L., Alonge, C., Wei, H., Meng, J., 2009. NLDAS Primary Forcing Data L4 Hourly 0.125× 0.125 Degree V002. Goddard Earth Sciences Data and Information Services Center (GES DISC), Greenbelt, MD, USA. https://doi.org/10.5067/6J5LHHOHZHN4. Rep. NASA/GSFC/HSI.
- Zan, C.S., Fyles, J.W., Girouard, P., Samson, R.A., 2001. Carbon sequestration in perennial bioenergy, annual corn and uncultivated systems in southern Quebec. Agric. Ecosyst. Environ. 86, 135–144. https://doi.org/10.1016/S0167-8809(00) 00273-5.

- Zhang, X., 2018. Simulating eroded soil organic carbon with the SWAT-C model. Environ. Model. Software 102, 39–48. https://doi.org/10.1016/j.envsoft.2018.01.005.
- Zhang, X., Izaurralde, R.C., Arnold, J.G., Sammons, N.B., Manowitz, D.H., Thomson, A. M., Williams, J.R., 2011. Comment on "modeling miscanthus in the soil and water assessment tool (SWAT) to simulate its water quality effects as a bioenergy crop.". Environ. Sci. Technol. 45, 6211–6212. https://doi.org/10.1021/es201463x.
- Zhang, X., Izaurralde, R.C., Arnold, J.G., Williams, J.R., Srinivasan, R., 2013. Modifying the Soil and Water Assessment Tool to simulate cropland carbon flux: model development and initial evaluation. Sci. Total Environ. 463–464, 810–822. https://doi.org/10.1016/j.scitotenv.2013.06.056.
- Zhang, X., Izaurralde, R.C., Manowitz, D., West, T.O., Post, W.M., Thomson, A.M., Bandaru, V.P., Nichols, J., Williams, J.R., 2010. An integrative modeling framework to evaluate the productivity and sustainability of biofuel crop production systems. GCB Bioenergy 2, 258–277. https://doi.org/10.1111/j.1757-1707.2010.01046.x.
- Zhang, X., Srinivasan, R., Van Liew, M., 2008. Multi-site calibration of the SWAT model for hydrologic modeling. Transactions of the ASABE 51, 2039–2049. https://doi. org/10.13031/2013.25407.
- Zhang, Y., Suyker, A., Paustian, K., 2018. Improved crop canopy and water balance dynamics for agroecosystem modeling using DayCent. Agron. J. 110, 511–524. https://doi.org/10.2134/agronj2017.06.0328.